Optical absorption spectra of intermediate-size silver clusters from first principles

Kopinjol Baishya, Juan C. Idrobo,* and Serdar Öğüt
Department of Physics, University of Illinois at Chicago, Chicago, Illinois 60607, USA

Mingli Yang and Koblar Jackson
Department of Physics, Central Michigan University, Mt. Pleasant, Michigan 48859, USA

Julius Jellinek
Chemical Sciences and Engineering Division, Argonne National Laboratory, Argonne, Illinois 60439, USA
(Received 30 May 2008; published 27 August 2008)

Optical absorption spectra of the three lowest-energy isomers of Ag_n ($n=10,12-20$) are investigated from first principles within the time-dependent local-density approximation (TDLDA). The computed spectra are found to be generally in good agreement with the available experimental data. The analyses of the spectra indicate that the *d* electrons of Ag_n clusters in this size range have a significant (70%–80%) contribution to low-energy optical excitations. We show that most of the peak positions and the relative intensities in the TDLDA spectra of these subnanometer sized clusters can be explained remarkably well within the classical Mie-Gans theory, using the dielectric function of bulk Ag and taking into account the shapes of the isomers.

DOI: 10.1103/PhysRevB.78.075439 PACS number(s): 78.67.−n, 36.40.Vz, 73.22.−f, 61.46.Bc

I. INTRODUCTION

Due to their intriguing physical and chemical properties, which are of particular relevance in catalysis, optoelectronics, and nanophotonics applications, noble-metal (Cu, Ag, Au) clusters and nanoparticles have been receiving a great deal of attention. Although the molecular orbitals or bands associated with the *d* electrons in these confined nanostructures are completely filled, their close energetic proximity to and spatial overlap with the *sp* states have important effects on their structural, electronic, and optical properties. A detailed understanding of these effects and how they influence the relevant materials' potentially useful and desirable properties are problems of fundamental and technological interest. One area, which has posed a computational challenge, is related to accurate modeling of the dielectric and optical properties of noble-metal clusters. For example, although the measured spectra for Ag_n ($n<40$) clusters embedded in rare-gas matrices have been available since the early 1990s, direct comparisons with predictions from reliable *ab initio* modeling techniques have lagged significantly.

The experimental optical spectra of Ag_n^+ ($n<21$) were first obtained via photofragmentation of mass selected clusters,[1] followed by measurements on matrix-embedded neutral Ag_n ($n<39$) clusters,[2–9] photodepletion spectroscopy of neutral and cationic clusters,[10,11] and photofragmentation of anionic clusters.[12] Recent progress in rare-gas matrix spectroscopy has resulted in new measurements on clusters of low abundance with significantly improved sensitivity.[13–16] Theoretically, *ab initio* optical properties of small Ag_n clusters ($n\leq 9$) were investigated by Bonačić-Koutecký *et al.* using quantum chemistry techniques.[9,17,18] Yabana and Bertsch[19] were the first to apply time-dependent density-functional theory (TDDFT) (Ref. 20) within the adiabatic local-density approximation (TDLDA) to Ag_n for the sizes $n=1,2,3,8$ using a real-space real-time approach. The application of TDDFT to Ag_n clusters was recently extended by us to sizes $n=1-8$ (Ref. 21), and 11 (Ref. 22), using *ab initio* pseudopotentials in a real-space frequency domain formalism,[23] resulting in good agreement with experimental data. More recently, Zhao *et al.* performed TDDFT calculations for Ag_4, Ag_6, and Ag_8 within an all-electron framework.[24] In addition, there have been recent applications of TDDFT to small Ag-Au (Ref. 25) and Ag-Ni (Ref. 26) nanoalloys. The role played by the *d* electrons in accurate predictions of absorption energies and oscillator strengths was emphasized in both the quantum chemistry and TDDFT studies.

In this paper, we continue with our TDLDA studies on Ag_n clusters extending their application to the intermediate ($n=10,12-20$) size region, allowing for a detailed, isomer-specific comparison of TDLDA optical spectra with available experimental data. Along with the computational studies in a very recent joint experimental/theoretical paper by Harb *et al.*,[16] the calculations presented here represent the first systematic TDDFT modeling studies performed from first principles on these relatively large Ag_n clusters. Our calculated optical absorption spectra are generally in good agreement with available experimental data and the results of Harb *et al.* We show that the *d* electrons of Ag_n clusters in the intermediate-size range have a significant contribution to optical excitations, reaching values as high as 70% for excitations below 3.5 eV and up to 80% below 6 eV. These percentages obtained for the $n=10-20$ size range are higher than those for the smaller Ag_n ($n\leq 8$) clusters. In spite of the significant direct involvement of the *d* electrons to the optical spectra, our analysis reveals that most of the peak positions and relative intensities obtained in our TDLDA studies can be explained remarkably well within the classical Mie-Gans theory,[27,28] using the dielectric function of bulk Ag and taking the shape of the isomers explicitly into account. This finding is particularly surprising given that the clusters considered here are in the subnanometer size range, much smaller than the typical size range to which this classical theory has traditionally been applied. The rest of the paper is organized as follows. In Sec. II, we present the theoretical

background and the computational parameters used in this study. The results and discussion for the structures, the optical absorption spectra, the angular characters of the optical excitations, and the comparisons with Mie-Gans theory are given in Sec. III. We conclude with a brief summary in Sec. IV.

II. THEORETICAL BACKGROUND AND COMPUTATIONAL METHODS

The Ag_n isomers considered in this study are the lowest-energy members of a pool of structures investigated at each size.[29] The candidate pool was obtained via an extensive, unbiased search for the ground-state structures of Cu_n clusters.[30] In that search, a large number (10^5-10^6) of conformations were sampled, and reduced to a group of 20–30 lowest-energy structures at each size through a hierarchical process involving successively more accurate theoretical models. The structures were fully relaxed to local minimum-energy configurations within density functional theory (DFT), using the Perdew-Burke-Ernzerhof gradient-corrected exchange-correlation functional.[31] To find the lowest-energy Ag_n isomers, the coordinates of this set of Cu_n structures were scaled by a factor of 1.18 (the ratio of the average Ag to Cu bond lengths for small clusters), and the Ag_n structures were relaxed within DFT. Limiting the Ag_n isomer search to the lowest-energy Cu_n structures is well justified, since the energy ordering of the Ag_n isomers was shown to be essentially the same as that of the corresponding Cu_n isomers.[29] In addition, the vertical ionization potentials computed for the ground-state structures[29] were found to be consistent with experimental measurements,[32] providing further evidence that the theoretical structures are the same as those sampled in the experiments.

Our calculations for the optical absorption spectra are performed using TDLDA and the frequency domain formalism of Casida.[20,23] The computations for the ground-state Kohn-Sham (KS) orbitals are carried out in real space within the framework of higher-order finite-difference *ab initio* pseudopotential method using the PARSEC code.[33] The scalar-relativistic pseudopotential used is the same as in Ref. 21. This electronic structure treatment, which is different from the one used to find the low-energy isomers, leads only to negligible changes in the bond lengths of the cluster structures. We solve the KS equations on three-dimensional Cartesian grids with uniform spacings of 0.45 to 0.5 a.u. inside large spherical domains of radii ranging from 28 to 32 a.u. depending on the size of the cluster. We use a Chebyshev-Davidson eigenvalue algorithm, and if an initial set of KS eigenpairs is known, by subspace filtering with Chebyshev polynomials.[34] We choose the total number of KS orbitals considered to be approximately 2.5 times larger than the number of occupied orbitals. These choices for the computational parameters lead to reliable and converged spectra up to 6 eV. The resulting dimensions for the KS Hamiltonian and the TDLDA matrices are $N \sim 10^6$ and $M \sim 5,000-18,000$, respectively. In the frequency domain formalism we employ a fast Fourier transform to calculate the direct (Coulomb) part of the TDLDA kernel. As such, in a TDLDA calculation for a given cluster, the computation of each of the $\sim M^2/2$ entries of the symmetric TDLDA matrix requires operations scaling as $N \log N$. Since Ag_n clusters with an odd number of atoms have an odd number of valence electrons, they call for spin-polarized treatments. We find though that the restricted (i.e., spin-unpolarized) formalism leads to no significant differences in the positions and intensities of the spectral lines. Therefore, the computations are performed using the restricted formalism. Further methodological and computational details can be found in Ref. 21.

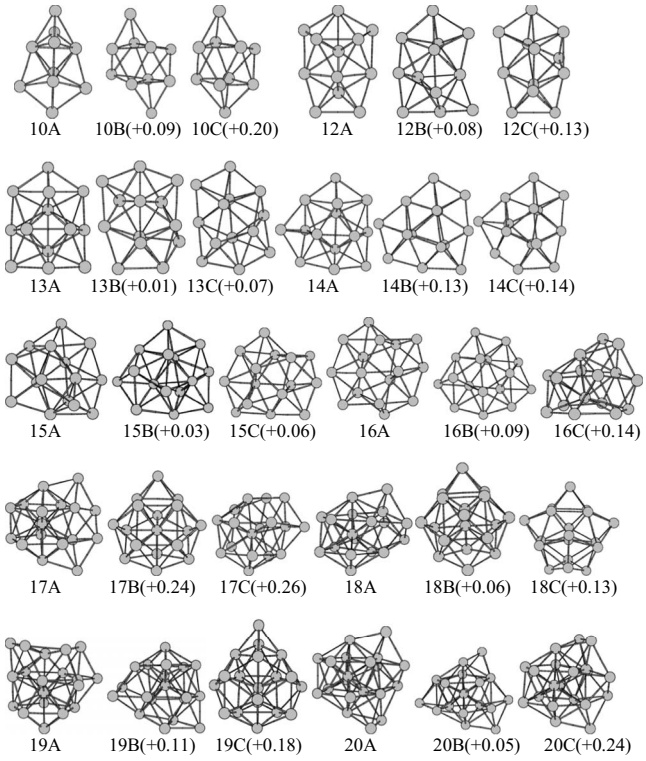

FIG. 1. Structures of the three lowest-energy isomers for Ag_n clusters $(n=10,12-20)$, ordered by energy with the lowest-energy structure (a) shown first at each size. The relative energies (in eV) of the higher-lying isomers with respect to structure A are shown in parentheses.

III. RESULTS AND DISCUSSION

A. Structures

The three lowest-energy isomers for Ag_n $(n=10,12-20)$ are shown in Fig. 1, along with their relative energies for each size. The atoms in each structure are closely packed and have large coordination numbers, but few specific bonding patterns are evident. There is a clear evolution in the shape of the structures, as noted in Ref. 29. For $n=10-15$, the structures have a layered character. For $n=10-13$, they are prolate or triaxial, while Ag_{14} and Ag_{15} are strongly oblate. At $n=16$, the two lowest-energy structures are layered and oblate, while the third isomer is more three dimensional. From $n=17$ to 20, the clusters become less and less oblate, and more spherical. Many of the structures can be described as having a 13-atom icosahedral core, with the remaining atoms

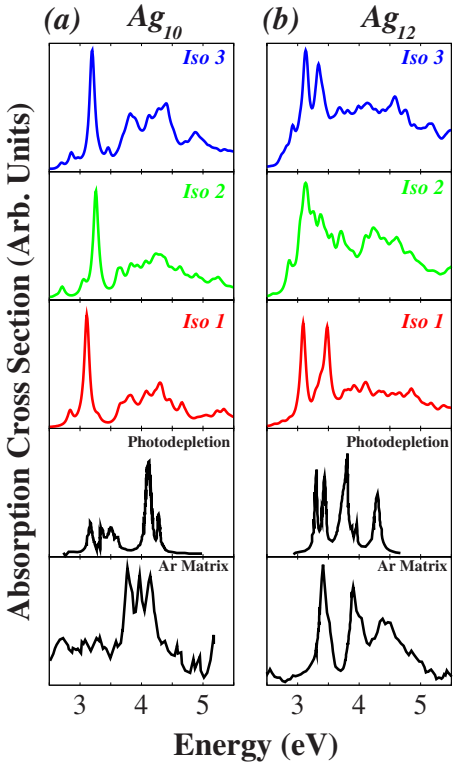

FIG. 2. (Color online) TDLDA spectra of Iso1, Iso2, and Iso3, along with absorption data from photodepletion (Ref. 11) and Ar-matrix spectroscopy (Refs. 14–16) experiments for (a) Ag_{10} and (b) Ag_{12}. The TDLDA spectra are broadened with Gaussians of width 0.05 eV.

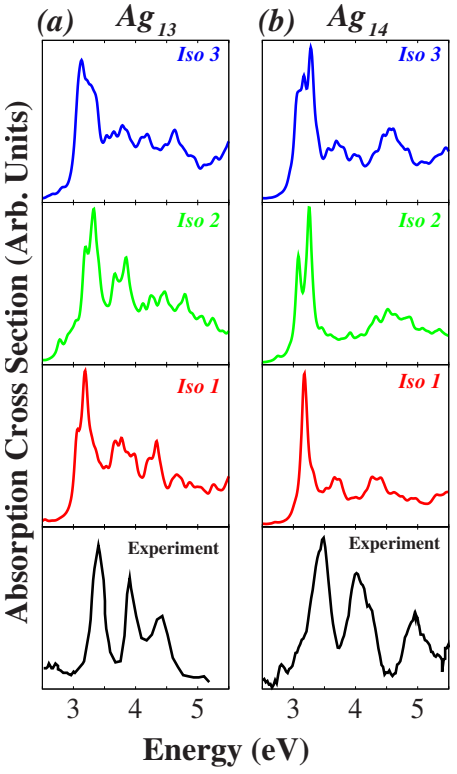

FIG. 3. (Color online) TDLDA spectra of Iso1, Iso2, and Iso3, along with absorption data from Ar-matrix spectroscopy (Refs. 15 and 16) experiments for (a) Ag_{13} and (b) Ag_{14}. The TDLDA spectra are broadened with Gaussians of width 0.05 eV.

decorating the surface. 17B, 18B, 18C, and 19C are exceptions having no icosahedral core. We note that the icosahedral Ag_{13} is quite high in energy, lying 0.86 eV above the calculated ground-state structure (13A) in Fig. 1. In addition, the double icosahedral structure for Ag_{19} lies 0.51 eV above structure 19A. More detailed information about the atomic and electronic structures of the Ag_n isomers can be found in Ref. 29.

B. TDLDA absorption spectra and comparison with experiment

The TDLDA optical absorption spectra for the three lowest-energy isomers (Iso1, Iso2, and Iso3) of Ag_n ($n=10,12-20$) along with experimental spectra[3–5,11,14–16] are plotted in Figs. 2–6 (for Ag_{11}, see Ref. 22). From the data presented in these figures, the following general observations can be made: (i) All calculated and experimental spectra exhibit sharp maxima near 3.5 eV, which slightly blueshift as n increases, (ii) with the exception of Ag_{10}, there is generally good agreement between the TDLDA spectra and the experimental data, and (iii) while more than one isomer could be contributing to the measured spectra at some sizes, the agreement with experiment is typically the best for the ground-state structure (Iso1), if the calculated spectra are blueshifted by up to ~0.5 eV. Regarding this last point, we note that when the energy differences between the isomers are small, as is the case for several sizes shown in Fig. 1, it is quite likely for different isomeric forms to get trapped inside the rare-gas matrix. In suggesting that more than one isomer might be represented in the measured spectrum, our main guiding criterion is the degree of similarity between the overall shapes of the measured and the computed spectra. As a secondary tool, we use blueshifts (which could be different for different sizes and isomers) in the comparison to account for the possible quantum confinement effects.[13,35] Below, we examine the calculated and experimental spectra for each size in more detail.

For Ag_{10} [Fig. 2(a)], the absorption data obtained by Conus *et al.*[14] in an Ar matrix at 28 K show three main peaks at 3.78, 3.97, and 4.15 eV. The lower-intensity peaks below 3.5 eV have been interpreted by Conus *et al.* as being most likely due to experimental artifacts. The photodepletion data of Rayner *et al.*, on the other hand, show an intense main peak at 4.15 eV and peaks of lower intensity at 3.15, 3.30, 3.50, 3.6, and 4.30 eV. Other than the common peak at 4.15 eV, the two experiments are not in good agreement with each other. Our computations for Iso1, Iso2, and Iso3 predict main peaks at 3.11, 3.26, and 3.20 eV, respectively, and series of secondary peaks beyond 3.6 eV. While the main peaks for all three isomers could perhaps be associated with the peaks near 3.15 and 3.30 eV obtained in the photodepletion study, it is clear that none of the theoretical spectra or their superpositions are in good agreement with either of the two experimental spectra. In their recent investigation,[16] Harb *et al.* also did not obtain good agreement between theory and experiment for Ag_{10}, and attributed this finding to the possible fragmenta-

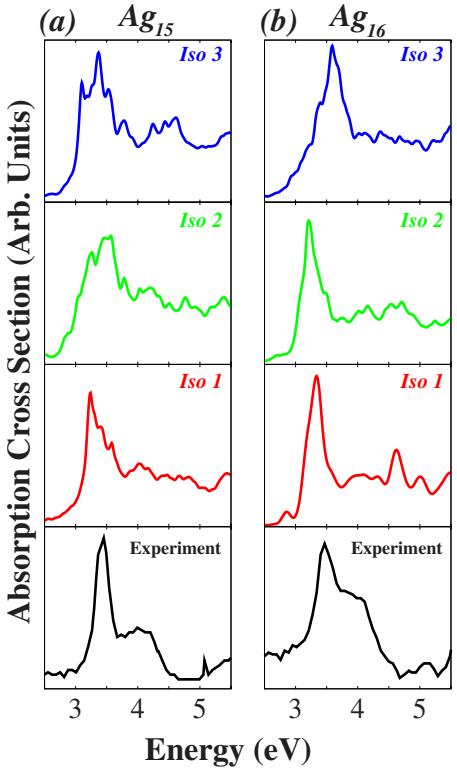

FIG. 4. (Color online) TDLDA spectra of Iso1, Iso2, and Iso3, along with absorption data from Ar-matrix spectroscopy (Ref. 3) experiments for (a) Ag_{15} and (b) Ag_{16}. The TDLDA spectra are broadened with Gaussians of width 0.05 eV.

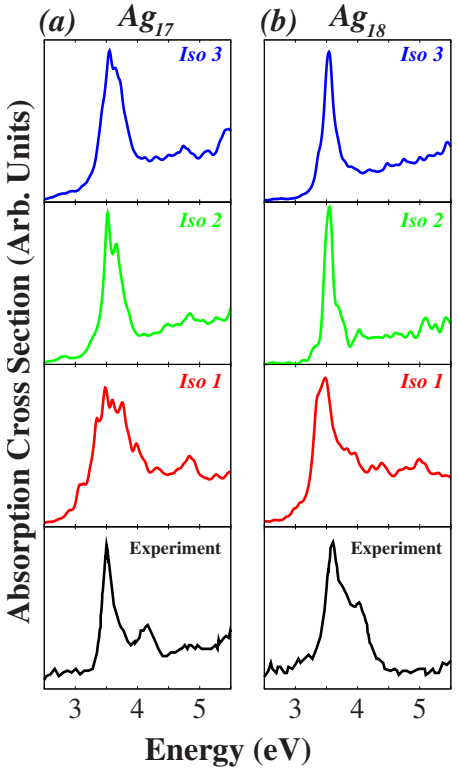

FIG. 5. (Color online) TDLDA spectra of Iso1, Iso2, and Iso3, along with absorption data from Ar-matrix spectroscopy (Ref. 3) experiments for (a) Ag_{17} and (b) Ag_{18}. The TDLDA spectra are broadened with Gaussians of width 0.05 eV.

tion of the Ag_{10} cluster into Ag_9 and an atom. Based on (i) the relatively high degree of agreement between experiment and theory obtained in the present study as well as the study of Harb *et al.* for the larger clusters, (ii) the low abundance of Ag_{10} in the mass spectrum, and (iii) the resemblance of the Ag_9 spectrum with the one reported for Ag_{10},[16] we believe that the fragmentation scenario suggested by Harb *et al.* for Ag_{10} is the most likely reason for the observed discrepancy.

The experimental results for the absorption spectrum of Ag_{12} from photodepletion[11] and Ar-matrix spectroscopy[15] studies are shown in Fig. 2(b) along with the TDLDA spectra for our three lowest-energy isomers. Other than slight shifts of the order of ~0.1 eV, the two experimental results are in good agreement with each other, consisting of three main peaks at 3.42, 3.91, and 4.38 eV (from Ar-matrix spectroscopy) with shoulders at slightly higher energies. Our TDLDA spectrum for Iso1 consists of two main peaks at 3.08 eV (oscillator strength $f=0.77$) and 3.48 eV ($f=0.67$) and broad features beyond 4 eV. Compared to Iso1, Iso2 has a similar absorption onset energy, a broader (rather than split) peak between 3.0 to 3.5 eV, and more enhanced transitions beyond 4 eV. The spectrum of Iso3 is quite similar to that of Iso1 with a slight reduction in the splitting of the first two peaks. If the TDLDA spectrum for Iso1 is blueshifted by ~0.4 eV, we obtain fairly good agreement with Ar-matrix absorption spectroscopy data regarding the relative intensities and splitting of the first two peaks. However, with similar blueshifts the contributions of Iso2 and Iso3 to the measured spectra cannot be ruled out. The large magnitude of the shift required to obtain this agreement suggests that quantum confinement due to the matrix probably plays an important role in the positions of the absorption peaks.[35]

For Ag_{13}, the experimental spectrum[16] obtained in an Ar matrix at 28 K consists of three main peaks at 3.40, 3.90, and 4.40 eV. As shown in Fig. 3(a), all three isomers have fairly good agreement with experimental data both in terms of the positions (within 0.1–0.2 eV) and the intensities of these three main peaks. Due to the striking similarity of the three spectra, it is not possible to tell if one or more of these isomers were present under the experimental conditions. Similar observations can be made about the spectra for Ag_{14} shown in Fig. 3(b). The experimental spectrum obtained in an Ar-matrix at 28 K consists of three main peaks at 3.49, 4.02, and 4.95 eV with decreasing intensity.[16] These can all be accounted for by corresponding peaks in the TDLDA spectra of Iso1 and possibly Iso3 by applying blueshifts of 0.3–0.5 eV (Iso1) and 0.2–0.35 eV (Iso3), resulting in a reasonable agreement between experiment and theory.

The experimental spectrum for Ag_{15} [Fig. 4(a)] consists of a main peak centered at 3.46 eV, followed by a broad shoulder from 3.7 to 4.5 eV, which Fedrigo *et al.* fitted to two Gaussians centered at 3.92 and 4.22 eV.[3] The main peaks for Iso1, Iso2, and Iso3 of Ag_{15} are observed at 3.24, 3.54, and 3.37 eV, respectively. While there are slight differences between the TDLDA spectra of the three isomers, all of them can be considered to capture the main features of the experimental spectrum. The measured spectrum for Ag_{16} [Fig.

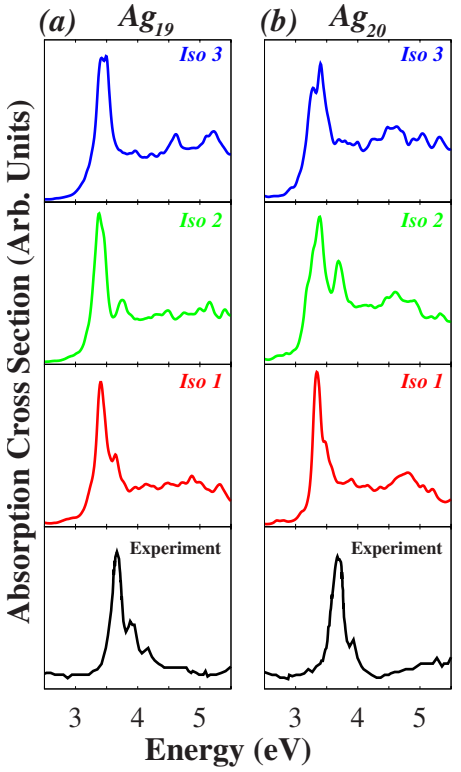

FIG. 6. (Color online) TDLDA spectra of Iso1, Iso2, and Iso3, along with absorption data from Ar-matrix spectroscopy (Ref. 3) experiments for (a) Ag_{19} and (b) Ag_{20}. The TDLDA spectra are broadened with Gaussians of width 0.05 eV.

4(b)] resembles that of Ag_{15} with a main peak centered at 3.50 eV and a broader shoulder which can be fitted to two Gaussians centered at 3.88 and 4.18 eV.[3] The main peaks for Iso1, Iso2, and Iso3 of Ag_{16} are observed at 3.33, 3.21, and 3.58 eV, respectively. The comparison between experiment and the TDLDA spectra suggests that Iso3 has a good overall agreement with experimental data without the need for a blueshift. The contributions from Iso1 and/or Iso2, however, cannot be ruled out.

For Ag_{17}, the experimental spectrum, shown in Fig. 5(a), exhibits a main peak at 3.52 eV followed by a smaller peak at 4.14 eV and a much weaker and broader feature near 4.8 eV. Taking only the first (main) peak into account, the TDLDA spectra for all three isomers have good agreement with experiment. On the other hand, it is not possible to assign the smaller experimental peak at 4.14 eV to any feature in the calculated spectra of Iso2 or Iso3, while it can be assigned to a combination of small peaks near 3.98 and 4.30 eV in the spectrum for Iso1. Based on this and the large energy difference (0.24 eV) between Iso1 and Iso2, we suggest Iso1 as the most likely cluster sampled under the experimental conditions. Similarly to Ag_{17}, the experimental spectrum of Ag_{18} [Fig. 5(b)] has a main peak at 3.62 eV followed by a smaller shoulder at 4.04 eV. The positions of the main peaks for Iso2 (3.55 eV) and Iso3 (3.54 eV) are in slightly better agreement with the experimental main peak. However, the overall shape of the spectrum for Iso1 (with a main peak at 3.49 eV and a shoulder at 3.93 eV), coincides almost perfectly with that of the experimental one, after applying a small (~0.1 eV) blueshift to the former. We, therefore, argue that although it is not possible to completely rule out the two higher-energy isomers, Iso1 is the most likely cluster sampled under the experimental conditions.

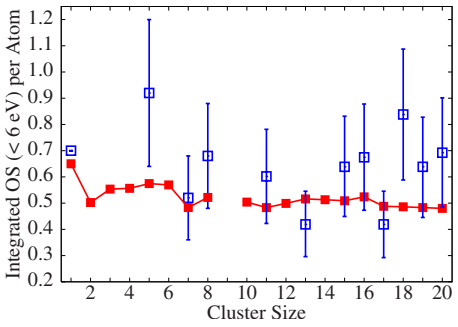

FIG. 7. (Color online) Integrated oscillator strengths (below 6 eV) per s electron of the lowest-energy Ag_n clusters as a function of n computed from the TDLDA spectra (red filled squares), along with estimates from experimental data (Refs. 2–4 and 36) (blue empty squares). The data for $n \leq 8$ and $n=11$ are from Refs. 21 and 22, respectively.

The experimental spectrum for Ag_{19} [Fig. 6(a)] consists of a main peak centered at 3.68 eV, followed by two smaller peaks of decreasing intensity at 3.91 and 4.15 eV. The calculated main peaks of Iso1, Iso2, and Iso3 are significantly redshifted with respect to the experimental peak and occur at 3.41, 3.38, and 3.46 eV, respectively. All three isomers exhibit secondary peaks at 3.64, 3.75, and 3.96 eV, respectively. Although the shape of the experimental spectrum matches best with the TDLDA spectrum of Iso1 (with a ~0.25 eV blueshift of the latter), it is quite possible that the experimental spectrum is composed of a superposition of the three spectra with some blueshift due to quantum confinement. Finally, the experimental spectrum of Ag_{20} [Fig. 6(b)] consists of a main peak at 3.70 eV followed by a smaller peak at 3.97 eV. Comparing this spectrum with those of the three isomers, we observe that the overall shape is best matched by the spectrum for Iso1, which exhibits the main peak at 3.35 eV and a shoulder at 3.48 eV, after a ~0.35 eV blueshift of the TDLDA spectrum.

Another comparison with the experimental data can be made in terms of the oscillator strengths. Figure 7 shows the integrated oscillator strengths (IOSs) per s electron as a function of the cluster size n for the lowest-energy structures. Optical transitions with energies below 6 eV are included. For completeness, we show the IOSs for all sizes we have worked with[21,22] up to $n=20$. The measured experimental values along with the corresponding error bars are also included.[2–4,36] The agreement with available experimental data is reasonable, with 10 out of 12 computed values in this size range falling within the experimental error bars. Overall, the IOSs per s electron for $n \leq 20$ are ~0.5, substantially reduced as compared to the case of alkali-metal clusters (where it is close to 1 per s electron). This reduction in the IOS is a consequence of the screening effect due to the d electrons.[21]

C. Orbital character of the optical excitations

In our previous studies on Ag_n ($n=2-8,11$) clusters, we showed that the d electrons affect the optical spectra by

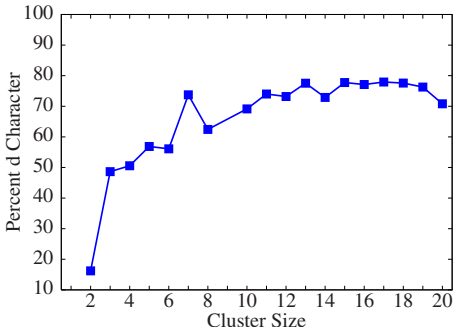

FIG. 8. (Color online) The percentage of the *d* character in the optical transitions calculated according to Eq. (1) for the computed ground-state structures of Ag_n as a function of n at the cutoff energy E_c=6 eV. The data for $n \leq 8$ and n=11 are from Refs. 21 and 22, respectively.

quenching the oscillator strengths and by getting partially involved in low-energy excitations. As before,[21,22,37] we quantify the role of the *d* electrons in the optical spectra by defining the percent of the *d* electron contributions integrated up to a cutoff energy E_c as

$$\%d = \frac{\sum_{i,\Omega_i<E_c} f_i \sum_{vc} |F_i^{vc}|^2 |\langle d|\phi_v\rangle|^2}{\sum_{i,\Omega_i<E_c} f_i} \times 100, \qquad (1)$$

where $\langle d|\phi_v\rangle$ is the l=2 component of the occupied orbital ϕ_v, f_i is the oscillator strength of the excitation at energy Ω_i, and the double index vc labels the entries of the corresponding TDLDA eigenvector F_i, which is composed of occupied-unoccupied (or "valence-conduction") Kohn-Sham orbital pairs. The degree of the integrated *d* character of the optical excitations for the ground-state structures of Ag_n clusters ($n \leq 20$) calculated in this fashion is shown as a function of size for the cutoff energy of E_c=6 eV in Fig. 8. We observe that the integrated *d* character increases almost monotonically with cluster size up to $n \sim 13$. In the intermediate ($10 \leq n \leq 20$) size range, the integrated *d* character of the optical excitations below 6 eV is approximately 70%–80%.

We also investigate how the integrated *s*, *p*, and *d* contributions[38] to the optical spectrum of a given cluster change as a function of the cutoff energy E_c. The variation of the percent of the *s*, *p*, and *d* electron contributions integrated up to E_c is shown as a function of E_c for the ground-state structures of Ag_{10}, Ag_{13}, and Ag_{20} in Figs. 9(a)–9(c). For Ag_{10}, the *d* character slowly rises above E_c=3.6 eV from ~35% to ~70% at E_c=6 eV, while the *sp* character decreases accordingly [Fig. 9(a)]. This shows that the first main peak in Iso1 of Ag_{10} at 3.11 eV [Fig. 2(a)] has mostly *sp* character with a small *d* admixture. For Ag_{13}, on the other hand, the *d* character jumps sharply from ~30% to ~70% within a very small energy range immediately above E_c =3 eV, approaching a value of near 80% at E_c=6 eV [Fig. 9(b)]. This shows that the first main peak in Iso1 of Ag_{13} [Fig. 3(a)] has a large *d* contribution. Ag_{20}, which exhibits a slight drop in the integrated *d* character at E_c=6 eV as a function of size (Fig. 8), shows a similar behavior in the

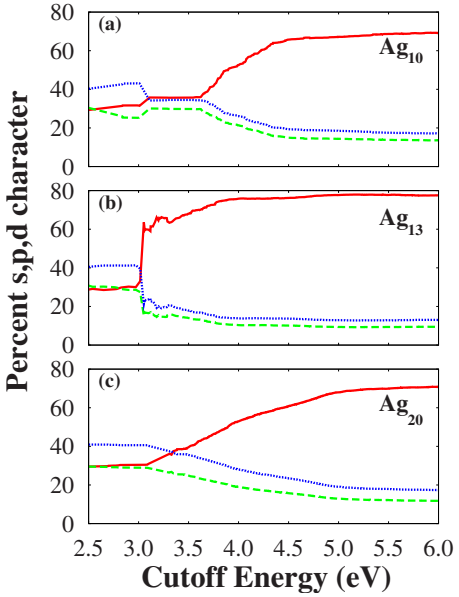

FIG. 9. (Color online) The percentages of the *s* (blue dotted lines), *p* (green dashed lines), and *d* (red solid lines) characters in the optical transitions for the ground-state structures of (a) Ag_{10}, (b) Ag_{13}, and (c) Ag_{20} as a function of the cutoff energy E_c.

orbital character of its excitations as a function of energy, rising slowly above 3.5 eV from ~35% to ~70% at E_c =6 eV. The main peak for Iso1 of Ag_{20} at 3.35 eV [Fig. 6(b)] has, therefore, mostly *sp* character.

The increase in the *d* character and the corresponding decrease in the *sp* character of the optical excitations as a function of E_c are actually in accord with the angular characters of the occupied Kohn-Sham orbitals. In Ag_n clusters, the molecular orbitals near the Fermi level E_F have mostly *sp* character, and orbitals of *d* character typically lie at more than ~3 eV below E_F.[39] Therefore, lowest-energy excitations are expected to be primarily associated with *sp* electrons. In addition, we observe that almost independent of the cluster size, the calculated angular characters averaged over all occupied states yield contributions of the *s*, *p*, and *d* type of ~7%, 4%, and 89%, respectively. These values are consistent with the *s*, *p*, and *d* characters of 1/11=9.1%, 0%, and 90.9% representative of the Ag atom. At very large cutoff energies, the *d* characters should, therefore, approach ~90%. This analysis shows that even though the *d* electron contributions integrated up to 6 eV can be as large as 70–80%, only a relatively small fraction of the *d* electrons have actually participated in the optical transitions up to this energy cutoff. For example, Ag_{20} has an IOS per atom value of 0.48 (Fig. 7) and an integrated *d* character of ~70% [Fig. 9(c)] at E_c=6 eV, which means that only $0.48 \times 0.7 = 0.336$ *d* electrons, or 3.36% of the total number of *d* electrons per atom, have been directly involved in the optical excitations up to E_c=6 eV, compared to $0.48 \times 0.3 = 0.144$ *s* electrons, which is 14.4% of the total number of *s* electrons per atom.

D. Comparison with predictions from Mie-Gans theory

In the early 1900s, Mie developed what is now a well-known classical theory, to explain the red color of tiny Au

particles in solution, by solving Maxwell's equations for electromagnetic waves interacting with small spherical metallic particles.[27] A few years thereafter, Gans extended the theory to ellipsoidal particles.[28] During the last two decades, this so-called Mie-Gans theory has been extensively used to interpret experimental data on light-matter interactions in large alkali and noble-metal nanoparticles with considerable success.[40–42] Recently, we have shown that the size independence and shape dependence of the overall features of the TDLDA spectra for *subnanometer* sized Si_n $(n=20-28)$ clusters can also be remarkably well explained within this classical theory using the bulk dielectric function of Si.[43] As for Ag_n clusters, after the first set of experimental data became available for them in the late 1980s,[44] various extensions of the Mie-Gans theory, which take into account the *d* electrons and the spill-out effects, were developed to explain the experimental observations.[1–3,5,45] Below, we compare our quantum-mechanical TDLDA spectra with predictions of the Mie-Gans theory using the dielectric function of bulk Ag and taking into account the shape of the cluster explicitly for these subnanometer sized Ag_n clusters.

For an ellipsoidal object in vacuum with semiaxes *A*, *B*, and *C*, the Mie-Gans theory, in the dipole approximation, gives the following expression for the absorption cross section:[41]

$$\sigma_{\rm abs}(\omega) = \frac{4\pi\omega ABC}{9c}\sum_{i=1}^{3}\frac{\epsilon_2(\omega)}{\{1+G_i[\epsilon_1(\omega)-1]\}^2+[G_i\epsilon_2(\omega)]^2}. \quad (2)$$

In this expression, $\epsilon_1(\omega)$ and $\epsilon_2(\omega)$ are the real and imaginary parts of the bulk dielectric function, *c* is the speed of light, and the depolarization factors G_i, which satisfy $\Sigma_{i=1}^{3}G_i=1$, are related to the shape of the ellipsoid. For prolate $(A=B<C)$ and oblate $(A=B>C)$ clusters, the corresponding depolarization factors satisfy $G_1=G_2>G_3$ and $G_1=G_2<G_3$, respectively, and can be directly calculated from the eccentricity of the spheroid.[40] For a spherical cluster, clearly $G_1=G_2=G_3=1/3$. Using the experimental dielectric function of bulk Ag, we show in Fig. 10 the Mie-Gans theory predictions for the absorption cross section (per atom) of silver clusters with prolate, spherical, and oblate geometry. For spheres, the Mie resonance (surface plasmon) occurs at 3.5 eV, strongly redshifted from the Drude model prediction of 5.2 eV due to the presence of semicore *d* electrons. For prolate clusters, the Mie resonance peak splits into two smaller peaks of roughly equal intensity; the amount of splitting is directly proportional to the degree of the prolateness of the cluster. For oblate clusters, the Mie resonance peak also splits into two by an amount proportional to the degree of the oblateness of the cluster; however, in this case the higher-energy peak has a much smaller amplitude than the lower-energy one, as shown in Fig. 10.

As discussed at the beginning of this section, there is a clear evolution in the shape of Ag_n clusters in the intermediate-size range. In order to quantify this size evolution and to compare cluster shapes more explicitly, we plot the normalized moments of inertia $\langle I_i\rangle = 3I_i/(I_1+I_2+I_3)$ for the calculated ground-state structures (Iso1) as a function of size in Fig. 11(a). The normalized moments directly indicate the cluster shape; in a spherical cluster, all three normalized moments are equal to unity; in a prolate (oblate) cluster, two moments are larger (smaller) than unity, and one moment is smaller (larger) than unity; in a triaxial $(A\neq B\neq C)$ cluster, all three moments are different from each other. Examination of the normalized moments in Fig. 11(a) shows that Ag_{20}

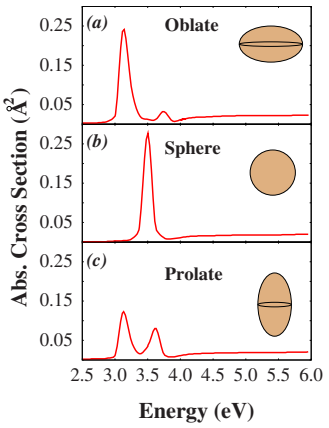

FIG. 10. (Color online) Predictions from Mie-Gans theory for the absorption cross section per atom (in $Å^2$) as a function of energy for (a) oblate, (b) spherical, and (c) prolate silver clusters.

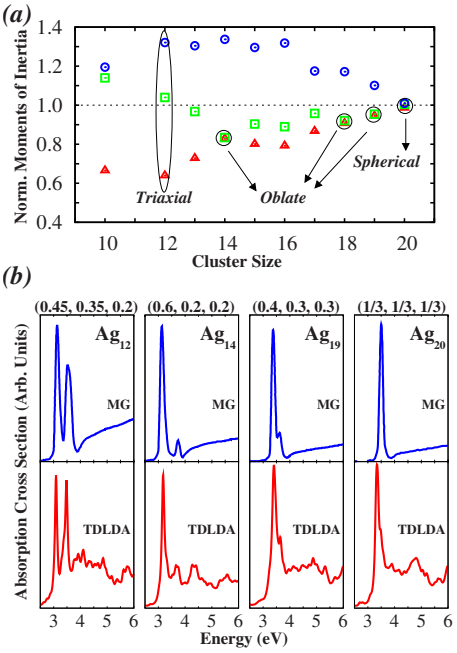

FIG. 11. (Color online) (a) Normalized moments of inertia $\langle I_i\rangle$ for the most stable structures (Iso1) of Ag_n showing examples of triaxial, oblate, and spherical clusters. (b) TDLDA absorption cross sections (red lines) and Mie-Gans (MG) theory predictions (blue lines) for triaxial Ag_{12}, oblate Ag_{14}, less oblate Ag_{19}, and spherical Ag_{20}. The three numbers in parentheses above each set of spectra for a given size are the G_1, G_2, G_3 depolarization factors used in plotting the Mie-Gans spectra, which are inferred from the geometries of the corresponding clusters.

with all three moments almost equal to 1 is near spherical, Ag_{14}, Ag_{18}, Ag_{19} are oblate (with decreasing degree of oblateness), and Ag_{12}, Ag_{13} are triaxial. With these observations about the shapes of the clusters and suitable corresponding choices for the depolarization factors G_i, we compare the TDLDA spectra with predictions of the Mie-Gans theory in Fig. 11(b). We note that the choices for the depolarization factors of different clusters are quite realistic. For example, in Ag_{14}, which is strongly oblate, we estimate the inequivalent semiaxis lengths C and A as 1.45 Å and 3.6 Å, respectively, resulting in an eccentricity of $e=\sqrt{1-(C/A)^2}\sim 0.92$. With this eccentricity for an oblate cluster, the depolarization factors are calculated[40] as $G_1=G_2=0.2$ and $G_3=0.6$.

As shown with four examples in Fig. 11, the agreement of quantum-mechanical TDLDA results with the classical Mie-Gans predictions using the bulk dielectric function of Ag is quite remarkable, given the fact that the clusters considered here are in the subnanometer size range. In the triaxial Ag_{12} cluster, the Mie-Gans theory, with suitable choices of G_i's, captures the two split TDLDA peaks quite well. For the oblate Ag_{14} and Ag_{19}, the relative heights of the first two TDLDA peaks are in good accord with the Mie-Gans predictions. Furthermore, in going from Ag_{14} to the less oblate Ag_{19}, we observe that the smaller TDLDA peak at the higher energy moves closer to the main peak at the lower energy, just as predicted by the Mie-Gans theory. Finally, for the nearly spherical Ag_{20}, the TDLDA spectrum is in good agreement with the Mie-Gans prediction of a single resonance, as the secondary peak has merged almost completely into the main peak at 3.5 eV.

IV. SUMMARY

We presented results on and analyses of the optical absorption spectra of the three lowest-energy isomers of Ag_n, $n=10,12-20$, obtained from first-principles calculations within time-dependent local-density approximation. Overall, our TDLDA spectra exhibit good agreement with the available experimental data. We find that the contributions of d electrons to optical spectra in this size range are higher (70%–80% for transitions below 6 eV) than those observed for smaller clusters. For certain sizes, the d electrons start to contribute considerably to optical spectra at energies as low as 3 eV. We show that the predictions of the classical Mie-Gans theory using the dielectric function of bulk Ag and the actual shapes of the isomers are in remarkably good agreement with quantum-mechanical TDLDA spectra, even in this subnanometer size range, *and* in the presence of significant d electron contribution to low-energy optical spectra.

ACKNOWLEDGMENTS

We would like to thank F. Conus and C. Félix for sharing with us their unpublished data on Ag_{12}, Ag_{13}, and Ag_{14}, and sending us their recent work[16] during the preparation of this manuscript. This work was supported by the U.S. Department of Energy Grants No. DE-FG02-03ER15488 (K.B., J.C.I., and S.Ö.), No. FG02-03ER15489 (M.Y. and K.J.), and the Office of Basic Energy Sciences, Division of Chemical Sciences, Geosciences, and Biosciences, under Contract No. DE-AC-02-06CH11357 (J.J.). This research used resources of NERSC, which is supported by the Office of Science of the U.S. Department of Energy.

*Present address: Department of Physics and Astronomy, Vanderbilt University, Nashville, Tennessee 37235.

[1] J. Tiggesbäumker, L. Köller, H. O. Lutz, and K. H. Meiwes-Broer, Chem. Phys. Lett. **190**, 42 (1992); J. Tiggesbäumker, L. Köller, K. H. Meiwes-Broer, and A. Liebsch, Phys. Rev. A **48**, R1749 (1993).

[2] W. Harbich, S. Fedrigo, and J. Buttet, Chem. Phys. Lett. **195**, 613 (1992).

[3] S. Fedrigo, W. Harbich, and J. Buttet, Phys. Rev. B **47**, 10706 (1993).

[4] S. Fedrigo, W. Harbich, J. Belyaev, and J. Buttet, Chem. Phys. Lett. **211**, 166 (1993).

[5] W. Harbich, Philos. Mag. B **79**, 1307 (1999).

[6] C. Félix, C. Sieber, W. Harbich, J. Buttet, I. Rabin, W. Schulze, and G. Ertl, Chem. Phys. Lett. **313**, 105 (1999).

[7] I. Rabin, W. Schulze, G. Ertl, C. Félix, C. Sieber, W. Harbich, and J. Buttet, Chem. Phys. Lett. **320**, 59 (2000).

[8] C. Félix, C. Sieber, W. Harbich, J. Buttet, I. Rabin, W. Schulze, and G. Ertl, Phys. Rev. Lett. **86**, 2992 (2001).

[9] C. Sieber, J. Buttet, W. Harbich, C. Félix, R. Mitrić, and V. Bonačić-Koutecký, Phys. Rev. A **70**, 041201(R) (2004).

[10] B. A. Collings, K. Athanassenas, D. M. Rayner, and P. A. Hackett, Chem. Phys. Lett. **227**, 490 (1994).

[11] D. Rayner, K. Athanassenas, B. A. Collings, S. Mitchell, and P. A. Hackett, in *Theory of Atomic and Molecular Clusters: With a Glimpse at Experiments*, edited by J. Jellinek (Springer, Berlin, 1999), p. 371.

[12] J. Tiggesbäumker, L. Köller, and K. H. Meiwes-Broer, Chem. Phys. Lett. **260**, 428 (1996).

[13] F. Conus, V. Rodrigues, S. Lecoultre, A. Rydlo, and C. Félix, J. Chem. Phys. **125**, 024511 (2006).

[14] F. Conus, J. T. Lau, V. Rodrigues, and C. Félix, Rev. Sci. Instrum. **77**, 113103 (2006).

[15] F. Conus and C. Félix (private communication).

[16] M. Harb, F. Rabilloud, D. Simon, A. Rydlo, S. Lecoultre, F. Conus, V. Rodrigues, and C. Félix (unpublished).

[17] V. Bonačić-Koutecký, J. Pittner, M. Boiron, and P. Fantucci, J. Chem. Phys. **110**, 3876 (1999).

[18] V. Bonačić-Koutecký, V. Veyret, and R. Mitrić, J. Chem. Phys. **115**, 10450 (2001).

[19] K. Yabana and G. F. Bertsch, Phys. Rev. A **60**, 3809 (1999).

[20] E. K. U. Gross, J. F. Dobson, and M. Petersilka, in *Density Functional Theory*, edited by R. F. Nalewajski (Springer-Verlag, Berlin, 1996), p. 81; M. Petersilka, U. J. Gossmann, and E. K. U. Gross, Phys. Rev. Lett. **76**, 1212 (1996); M. E. Casida, in *Recent Advances in Density Functional Methods*, edited by D. P. Chong (World Scientific, Singapore, 1995), Pt. I, p. 155; *Recent Developments and Applications of Modern Density Functional*

Theory, edited by J. M. Seminario (Elsevier, Amsterdam, 1996), p. 91; K. Burke, M. Petersilka, and E. K. U. Gross, in *Recent Advances in Density Functional Methods*, edited by P. Fantucci and A. Bencini (World Scientific, Singapore, 2002), Vol. III, p. 67.

[21] J. C. Idrobo, S. Öğüt, and J. Jellinek, Phys. Rev. B **72**, 085445 (2005); **77**, 239901(E) (2008).

[22] J. C. Idrobo, S. Öğüt, K. Nemeth, J. Jellinek, and R. Ferrando, Phys. Rev. B **75**, 233411 (2007).

[23] I. Vasiliev, S. Öğüt, and J. R. Chelikowsky, Phys. Rev. Lett. **82**, 1919 (1999); Phys. Rev. B **65**, 115416 (2002).

[24] G. F. Zhao, Y. Lei, and Z. Zeng, Chem. Phys. **327**, 261 (2006).

[25] F. Y. Chen and R. L. Johnston, Appl. Phys. Lett. **90**, 153123 (2007).

[26] M. Harb, F. Rabilloud, and D. Simon, J. Phys. Chem. A **111**, 7726 (2007).

[27] G. Mie, Ann. Phys. **25**, 377 (1908); C. Bohren and D. Huffman, *Absorption and Scattering of Light by Small Metallic Particles* (Wiley, New York, 1983).

[28] R. Gans, Ann. Phys. **37**, 881 (1912).

[29] M. Yang, K. A. Jackson, and J. Jellinek, J. Chem. Phys. **125**, 144308 (2006).

[30] M. Yang, K. A. Jackson, C. Koehler, Th. Frauenheim, and J. Jellinek, J. Chem. Phys. **124**, 024308 (2006).

[31] J. P. Perdew, K. Burke, and M. Ernzerhof, Phys. Rev. Lett. **77**, 3865 (1996).

[32] C. Jackschath, I. Rabin, and W. Schulze, Z. Phys. D: At., Mol. Clusters **22**, 517 (1992).

[33] J. R. Chelikowsky, N. Troullier, and Y. Saad, Phys. Rev. Lett. **72**, 1240 (1994).

[34] Y. Zhou, Y. Saad, M. L. Tiago, and J. R. Chelikowsky, Phys. Rev. E **74**, 066704 (2006).

[35] B. Gervais, E. Giglio, E. Jacquet, A. Ipatov, P.-G. Reinhard, and E. Suraud, J. Chem. Phys. **121**, 8466 (2004); B. Gervais, E. Giglio, E. Jacquet, A. Ipatov, P.-G. Reinhard, F. Fehrer, and E. Suraud, Phys. Rev. A **71**, 015201 (2005).

[36] E. Moore, *Atomic Energy Levels*, Natl. Bureau Standards, Circ. No. 467 (U.S. GPO, Washington, D.C., 1958), Vol. III; N. P. Penkin and I. Yu. Slavenas, Opt. Spektrosk. **15**, 9 (1963).

[37] J. C. Idrobo, W. Walkosz, S. F. Yip, S. Öğüt, J. Wang, and J. Jellinek, Phys. Rev. B **76**, 205422 (2007); **77**, 249903(E) (2008).

[38] We use Eq. (1) to compute the integrated *s*, *p*, and *d* contributions by taking the $l=0$, 1, and 2 angular momentum components, respectively, of the occupied orbital. The results presented in Fig. 9 are normalized such that the *s*, *p*, and *d* contributions add up to 100%. This is an excellent approximation, as the sums before normalization are typically above 95%.

[39] M. Pereiro and D. Baldomir, Phys. Rev. A **75**, 033202 (2007).

[40] A. Heilmann, M. Quinten, and J. Werner, Eur. Phys. J. B **3**, 455 (1998).

[41] S. Link and M. A. El-Sayed, Int. Rev. Phys. Chem. **19**, 409 (2000).

[42] K. Selby, M. Vollmer, J. Masui, V. Kresin, W. A. de Heer, and W. D. Knight, Phys. Rev. B **40**, 5417 (1989); I. A. Solov'yov, A. V. Solv'yov, and W. Greiner, J. Phys. B **37**, L137 (2004).

[43] J. C. Idrobo, M. Yang, K. A. Jackson, and S. Öğüt, Phys. Rev. B **74**, 153410 (2006).

[44] K. P. Charlé, W. Schulze, and B. Winter, Z. Phys. D: At., Mol. Clusters **12**, 471 (1989).

[45] V. V. Kresin, Phys. Rev. B **51**, 1844 (1995).